

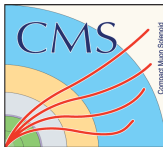
Evidence for off-shell Higgs boson production and the measurement of its width

Mostafa Mahdavihorrani^{1,2} on behalf of the CMS collaboration

¹ Université Libre de Bruxelles and IIHE

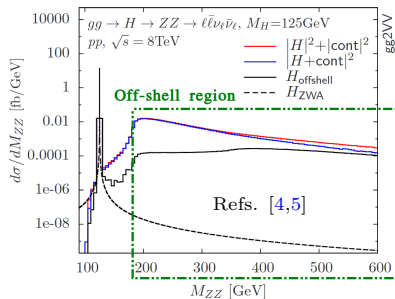
² University of Antwerp

October 20, 2021



H \rightarrow ZZ \rightarrow 2 ℓ 2 ν analysis (HIG-21-013)

- In this analysis ([Analysis PAS: HIG-21-013](#)) we study the off-shell Higgs production in H \rightarrow ZZ \rightarrow 2 ℓ 2 ν signal channel (ggH and VBF) where $\ell = e, \mu$. The analysis is based on Data collected by CMS experiment during LHC run 2 (2016-2018) at $\sqrt{s} = 13$ TeV and with integrated luminosity of $\sim 138\text{fb}^{-1}$.
- Goals:
 - Measuring of signal strength parameters ($\mu^{\text{off-shell}}$, $\mu_{\text{F}}^{\text{off-shell}}$, $\mu_{\text{V}}^{\text{off-shell}}$) \Rightarrow off-shell 2 ℓ 2 ν results are combined with 4 ℓ off-shell analysis [1]
 - Measuring Γ_{H} and constraining anomalous couplings strengths (f_{ai}) \Rightarrow off-shell 2 ℓ 2 ν results are combined with 4 ℓ on-shell analyses [2,3].
- Signal and interfering backgrounds (MELA reweighting)
- $q\bar{q} \rightarrow \text{ZZ(WZ)}$ backgrounds (simulation + 3 ℓ WZ CR)
- Instrumental $p_{\text{T}}^{\text{miss}}$ from DY (data-driven + γ CR)
- Nonresonant backgrounds (data-driven + $e\mu$ CR)
- Other minor backgrounds (simulation)



*** MELA = Matrix Element Likelihood Analysis, CR = Control Region, DY = Drell-Yan ***

Likelihood scans of signal strengths and Γ_H

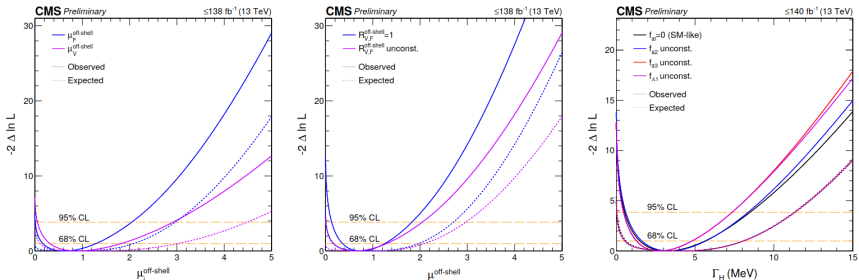


Figure 1: Observed (solid) and expected (dashed) likelihood scans for $\mu_F^{\text{off-shell}}$ or $\mu_V^{\text{off-shell}}$ (left), $\mu_F^{\text{off-shell}}$ (middle), and Γ_H (right). Scans for $\mu_F^{\text{off-shell}}$ (blue) and $\mu_V^{\text{off-shell}}$ (magenta) are obtained with the other parameter unconstrained. Those for $\mu_F^{\text{off-shell}}$ are shown with (blue) and without (magenta) the constraint $R_{V,F}^{\text{off-shell}} = 1$. Constraints on Γ_H are shown with and without anomalous HVV couplings. The horizontal lines indicate the 68% and 95% CL regions.

Summary of results

Table 1: Summary of results on the off-shell signal strength and Γ_H . Results for $\mu^{\text{off-shell}}$ are with $R_{V,F}^{\text{off-shell}}$ either unconstrained or = 1. Constraints on $\mu_F^{\text{off-shell}}$ and $\mu_V^{\text{off-shell}}$ are shown with the other signal strength unconstrained. Results for Γ_H (in units of MeV) are obtained with the on-shell signal strengths unconstrained. Tests with anomalous HVV couplings are distinguished by the denoted on-shell cross section fractions. The expected values (not shown) are either unity or $\Gamma_H = 4.1$ MeV. The abbreviation ‘c.v.’ stands for ‘central value’, and the abbreviation ‘(u)’ stands for ‘unconstrained’.

| Param. | Cond. | Observed | | Expected | |
|-----------------------|-----------------------------|----------|-----------------------------|---|--|
| | | c.v. | 68% 95% CL | 68% 95% CL | |
| $\mu_F^{\text{off.}}$ | $\mu_V^{\text{off.}}$ (u) | 0.62 | [0.17, 1.3] [0.0060, 2.0] | $[2 \cdot 10^{-5}, 2.1]$ < 3.0 | |
| $\mu_V^{\text{off.}}$ | $\mu_F^{\text{off.}}$ (u) | 0.90 | [0.31, 1.8] [0.051, 2.9] | $[0.11, 3.0]$ < 4.5 | |
| $\mu^{\text{off.}}$ | $R_{V,F}^{\text{off.}} = 1$ | 0.74 | [0.36, 1.3] [0.13, 1.8] | $[0.16, 2.0]$ $[0.0086, 2.7]$ | |
| | $R_{V,F}^{\text{off.}}$ (u) | 0.62 | [0.17, 1.3] [0.0061, 2.0] | $[4 \cdot 10^{-5}, 2.1]$ $[1 \cdot 10^{-5}, 3.0]$ | |
| Γ_H | SM-like | 3.2 | [1.5, 5.6] [0.53, 8.5] | $[0.62, 8.1]$ $[0.035, 11.3]$ | |
| Γ_H | f_{a2} (u) | 3.4 | [1.6, 5.7] [0.60, 8.4] | $[0.52, 8.0]$ $[0.015, 11.3]$ | |
| Γ_H | f_{a3} (u) | 2.7 | [1.3, 4.8] [0.47, 7.3] | $[0.53, 8.0]$ $[0.015, 11.3]$ | |
| Γ_H | $f_{\Lambda 1}$ (u) | 2.7 | [1.3, 4.8] [0.46, 7.2] | $[0.55, 8.1]$ $[0.019, 11.3]$ | |

Results interpretations on BSM HVV couplings

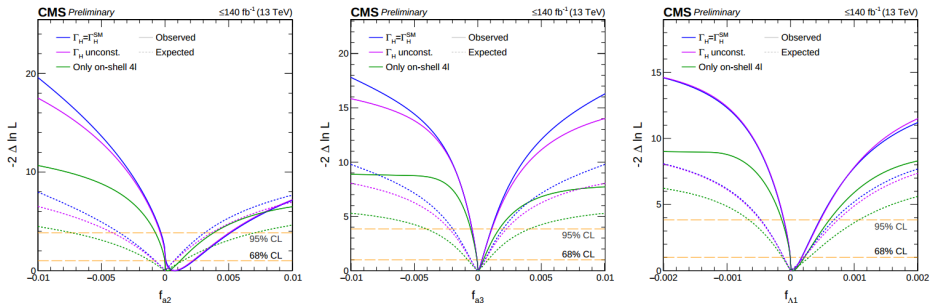


Figure 6: Shows the likelihood scans of f_{a2} (left), f_{a3} (middle), and $f_{\Lambda 1}$ (right) are shown with the constraint $\Gamma_H = \Gamma_H^{\text{SM}}$ (blue), Γ_H unconstrained (violet), or based on on-shell 4ℓ only (green). Observed (expected) scans are shown with solid (dashed) curves. The horizontal lines indicate the 68% and 95% CL regions.

Backup

Table 2: Comparisons between the number of observed events in the $2\ell 2\nu$ channel with expectations from the SM and no-off-shell scenarios as a function of N_j for low and high m_T^{ZZ} . An additional requirement of $p_T^{\text{miss}} \geq 200$ GeV has been imposed for $N_j \geq 2$.

| | m_T^{ZZ} | $N_j = 0$ | $N_j = 1$ | $N_j \geq 2$ |
|---------|----------------|--------------------|-------------------|----------------|
| SM | < 450 GeV | 1118^{+45}_{-49} | 660^{+31}_{-40} | 92^{+7}_{-8} |
| No off. | < 450 GeV | 1127^{+46}_{-49} | 666^{+31}_{-40} | 93^{+7}_{-8} |
| Data | < 450 GeV | 989 | 643 | 95 |
| SM | ≥ 450 GeV | 241^{+13}_{-14} | 166^{+10}_{-12} | 68^{+5}_{-6} |
| No off. | ≥ 450 GeV | 252^{+14}_{-14} | 178^{+10}_{-13} | 75^{+5}_{-6} |
| Data | ≥ 450 GeV | 217 | 151 | 66 |

Sensitivity of off-shell $2\ell 2\nu$ channel, CMS

Table 4: Constraints on the $\mu_F^{\text{off-shell}}$, $\mu_V^{\text{off-shell}}$, and $\mu^{\text{off-shell}}$ parameters are summarized. The constraints on $\mu^{\text{off-shell}}$ are obtained with $R_{V,F}^{\text{off-shell}}$ unconstrained or = 1. The measurements are presented using the $2\ell 2\nu$ analysis alone, or with the inclusion of off-shell 4ℓ events. The designation ‘c.v.’ stands for the central value obtained in the likelihood scan, and the expected central value is always unity, so it is not quoted explicitly.

| Parameter | Condition | c.v. | Observed | | Expected | |
|--|---------------------------------------|------|---|--------|---|--------|
| | | | 68% | 95% CL | 68% | 95% CL |
| $\mu_F^{\text{off-shell}}$ ($2\ell 2\nu + 4\ell$) | $\mu_V^{\text{off-shell}}$ unconst. | 0.62 | [0.17, 1.3] [0.0060, 2.0] | | $[2 \cdot 10^{-5}, 2.1]$ < 3.0 | |
| $\mu_F^{\text{off-shell}}$ ($2\ell 2\nu$) | $\mu_V^{\text{off-shell}}$ unconst. | 0.41 | [0.014, 1.4] < 2.6 | | < 2.5 < 3.7 | |
| $\mu_V^{\text{off-shell}}$ ($2\ell 2\nu + 4\ell$) | $\mu_F^{\text{off-shell}}$ unconst. | 0.90 | [0.31, 1.8] [0.051, 2.9] | | [0.11, 3.0] < 4.5 | |
| $\mu_V^{\text{off-shell}}$ ($2\ell 2\nu$) | $\mu_F^{\text{off-shell}}$ unconst. | 1.1 | [0.28, 2.4] [0.016, 3.8] | | [0.07, 3.2] < 4.8 | |
| $\mu^{\text{off-shell}}$ ($2\ell 2\nu + 4\ell$) | $R_{V,F}^{\text{off-shell}} = 1$ | 0.74 | [0.36, 1.3] [0.13, 1.8] | | [0.16, 2.0] [0.0086, 2.7] | |
| | $R_{V,F}^{\text{off-shell}}$ unconst. | 0.62 | [0.17, 1.3] [0.0061, 2.0] | | $[4 \cdot 10^{-5}, 2.1]$ $[1 \cdot 10^{-5}, 3.0]$ | |
| $\mu^{\text{off-shell}}$ ($2\ell 2\nu$) | $R_{V,F}^{\text{off-shell}} = 1$ | 0.74 | [0.25, 1.5] [0.043, 2.3] | | [0.11, 2.3] $[2 \cdot 10^{-4}, 3.2]$ | |
| | $R_{V,F}^{\text{off-shell}}$ unconst. | 0.41 | [0.014, 1.4] $[2 \cdot 10^{-5}, 2.6]$ | | $[3 \cdot 10^{-5}, 2.5]$ $[6 \cdot 10^{-6}, 3.7]$ | |

Table 10: Summary of allowed 68% CL (central values with uncertainties) and 95% CL (in square brackets) intervals for $\mu^{\text{off-shell}}$, $\mu_{\text{F}}^{\text{off-shell}}$, and $\mu_{\text{V}}^{\text{off-shell}}$ obtained from the analysis of the combination of Run 1 and Run 2 off-shell data sets.

| Parameter | Observed | Expected |
|-------------------------------------|-------------------------------------|-----------------------------------|
| $\mu^{\text{off-shell}}$ | $0.78^{+0.72}_{-0.53} [0.02, 2.28]$ | $1.00^{+1.20}_{-0.99} [0.0, 3.2]$ |
| $\mu_{\text{F}}^{\text{off-shell}}$ | $0.86^{+0.92}_{-0.68} [0.0, 2.7]$ | $1.0^{+1.3}_{-1.0} [0.0, 3.5]$ |
| $\mu_{\text{V}}^{\text{off-shell}}$ | $0.67^{+1.26}_{-0.61} [0.0, 3.6]$ | $1.0^{+3.8}_{-1.0} [0.0, 8.4]$ |

[arXiv:1901.00174](https://arxiv.org/abs/1901.00174)

Table 2: The 95% CL upper limits on $\mu_{\text{off-shell}}$, $\Gamma_H/\Gamma_H^{\text{SM}}$ and R_{gg} . Both the observed and expected limits are given. The 1σ (2σ) uncertainties represent 68% (95%) confidence intervals for the expected limit. The upper limits are evaluated using the CL_s method, with the SM values as the alternative hypothesis for each interpretation.

| | | Observed | Median | Expected | |
|---------------------------------|--------------------------------------|----------|--------|---------------|---------------|
| | | | | $\pm 1\sigma$ | $\pm 2\sigma$ |
| $\mu_{\text{off-shell}}$ | $ZZ \rightarrow 4\ell$ analysis | 4.5 | 4.3 | [3.3, 5.4] | [2.7, 7.1] |
| | $ZZ \rightarrow 2\ell 2\nu$ analysis | 5.3 | 4.4 | [3.4, 5.5] | [2.8, 7.0] |
| | Combined | 3.8 | 3.4 | [2.7, 4.2] | [2.3, 5.3] |
| $\Gamma_H/\Gamma_H^{\text{SM}}$ | Combined | 3.5 | 3.7 | [2.9, 4.8] | [2.4, 6.5] |
| R_{gg} | Combined | 4.3 | 4.1 | [3.3, 5.6] | [2.7, 8.2] |

[arXiv:1808.01191v2](#)

Most of the systematics affect both the shape and normalization

- Theoretical uncertainties:

- Renormalization scale and Factorization scale (up to 30%)
- $\alpha_S(m_Z)$ and PDF variations (up to 20%)
- Simulation of the second jet in gg samples (up to 20%)
- Scale and tune variations of PYTHIA
- NLO EW correction ($q\bar{q} \rightarrow ZZ, WZ$)
- Uncorrelated uncertainties on $N_j = 0$ (2.7%), $N_j = 1$ (6.0%) and $N_j \geq 2$ (7.6%) in $q\bar{q} \rightarrow ZZ, WZ$ derived from the 3 ℓ CR

- Instrumental uncertainties on the simulations:

- Luminosity (between 1.2% and 2.5%, depending on the data taking period)
- L1 prefire scale
- Pile-up, JES, JER and p_T^{miss} resolution correction
- Uncertainties in lepton, trigger, pile-up jet identification, and b-tagging efficiencies (typically 1% per lepton)

Statistical uncertainties on simulations are also taken into account.